Estimation of effective plant area index using LiDAR data in forest of South Korea

Doo-Ahn Kwak[1], Woo-Kyun Lee[1] & Hyun-Kook Cho[2]

[1] Division of Environmental Science and Ecological Engineering, Korea University, Seoul 136-701, South Korea, leewk@korea.ac.kr
[2] Department of Forest Resource Information, Korea Forest Research Institute, Seoul 136-012, South Korea, hcho@forest.go.kr

Abstract

The Effective Plant Area Indices (PAI_e) of *Pinus koraiensis*, *Larix leptolepis* and *Quercus* spp. were estimated by calculating the laser-intercepted rate through the forest canopy using LiDAR data. Initially, the Laser Interception Index (LII), which is related to the canopy gap fraction, was generated by extracting the LiDAR data reflected through the canopy using *k*-means statistics. The LiDAR-derived PAI_e was then estimated by applying LII to the Beer-Lambert law. From a comparison of the LiDAR-derived to the field-derived PAI_e, the coefficients of the determination by the tree species was 0.82, 0.71 and 0.54 for *Pinus koraiensis*, *Larix leptolepis* and *Quercus* spp., respectively. The change in accuracy according to the tree species was attributed to the density of leaves and understory, the interference by stems, the amount of leaves and the vertical number of branches in the forest stands. From field estimations at the time of the study, *Pinus koraiensis* had dense leaves and *Larix leptolepis* had dense branches, while *Quercus* spp. had no leaves or a few big branches. This can be explained by the estimation of the field-derived PAI_e being influenced by the stem shadow and direct sunlight due to the few leaves and poor branches in the *Quercus* spp. stand surveyed, even though the estimation of the LiDAR-derived PAI_e was hardly affected by them.

Keywords: Leaf Area Index, Plant Area Index, LiDAR, Laser Interception Index, k-means clustering

1. Introduction

According to Jonckheere *et al*. (2004), there are several definitions for the LAI used in the field, which can be defined as the total one-sided area of leaf tissue per unit ground surface area (Watson, 1947). Schulze *et al*. (2005) suggested that the LAI could be determined by the sum of the projected leaf surface per soil area. On the other hand, Myneni *et al*. (1997) defined the LAI as the maximum projected leaf area per unit ground surface area. Such variously defined LAI can be derived from both the within and below canopy microclimate, control canopy water interception and radiation extinction, as well as water and carbon gas exchange (Bréda, 2003). Moreover, they provide information for biosphere modelling (Bonan, 1993) because they contain information on a number of relevant ecological process (Morsdorf *et al*., 2006). Therefore, the LAI can play a key role within biogeochemical cycles in an ecosystem. The various methods for obtaining the LAI can be classified into two categories; direct and indirect measurements (Bréda, 2003). Direct methods are destructive and exhaustive due to harvesting vegetation. Moreover, such methods are time-consuming and labour-intensive when the LAI is obtained from field measurements. Thereby, the direct methods are suitable for vegetation with small structures, but are difficult to apply to large areas or trees (Bréda, 2003). On the other hand, the LAI by indirect and non-destructive methods can be easily estimated using the radiative characteristics of sunlight, which is dispersed or penetrates through the vegetation area. With such methods, remote sensing techniques, using satellite imagery and aerial photography,

have been applied to derive this measurement. Many such approaches are based on passive optical sensor systems and regression models (Cohen *et al*., 2003) or radiative transfer modelling (Koetz *et al*., 2004). However, one serious problem with remote sensing using passive sensor systems is that they are unable to describe the canopy shape and structure, and the vertical distribution of leaves because they do not contain the elevation information by itself. Light Detection and Ranging (LiDAR), especially using an active sensor system, has recently been used to extract surface information, and can acquire highly accurate object shape characteristics using geo-registered 3D-points (Kwak *et al*., 2007). The LiDAR system can measure both vertical and horizontal forest structures, such as the tree heights, sub-canopy topographies and distributions in forested areas with high precision (Holmgren *et al*., 2003). Such characteristics can be used to extract forest information. Morsdorf *et al*., (2006) derived the LAI using fCover (fractional cover) and Riãno *et al.* (2004) obtained the LAI using the gap fraction distribution. Koetz *et al*. (2006) applied the LiDAR waveform model to generate the fCover and LAI from large footprint LiDAR data. However, it is difficult for large footprint LiDAR to extract forest information in small areas. The use of ground based laser scanners is limited by the topographical conditions of the study area as well as to small forest areas not broad forest areas. Barilotti *et al*. (2006) suggested an estimation of the LAI using the Laser Penetration Index (LPI) generated by the point density of LiDAR data, according to the penetration of a laser beam through the canopy of forested areas. However, the threshold value between the transmission and reflectance through the canopy cannot be applied to another forest stand, including fluctuant height understory, because the value was fixed to a height 1 m above the ground.

For such an indirect LAI estimation, a common method in the field is to use an optical sensor to acquire photosynthetically active radiation (PAR) using an AccuPAR-80 Linear PAR/LAI Ceptometer of Decagon Devices, LAI-2000 or hemispherical photography below the canopy (Pocewicz *et al*., 2004). However, the values recorded with such instruments are not pure LAIs because clumping of the canopy components and the influence of individual tree stems and woody canopy components are not adjusted for (Pocewicz *et al*., 2004). The value recorded without the consideration of clumping of the canopy components is defined as the effective LAI (LAI_e). Measurements that do not consider light interception by woody components are called the plant area index (PAI), and, if no adjustments are made for the clumping of canopy elements, the values measured by the instruments are referred to as the effective PAI (PAI_e). Therefore, the values measured with optical sensors in forest areas is almost the PAI_e (Pocewicz *et al*., 2004).

Chen and Cihlar (1996) reported that the PAI_e estimation was more effective in representing the vegetation indices than the LAI estimation because the PAI_e could represent the sunlight interception well by the woody canopy elements and individual tree stems. Therefore, in this study, to approximate the LAI, the PAI_e of *Pinus koraiensis*, *Larix leptolepis* and *Quercus* spp. were estimated by calculating the rate of laser-intercepted LiDAR points through the canopy using LiDAR data. In particular, for the approximate LAI, an attempt was made to estimate only the PAI_e of the canopy part as classifying the LiDAR pulses reflected in forest stands into in- and below-canopy returns using the *k*-means clustering method.

2. Study area

The study areas were located in the Gwangneung Experimental Forest of the Korea Forest Research Institute (the upper left 127°7′30.72523″E, 37°48′0.42761″N and lower right 127°11′59.17548″E, 37°41′59.31795″N), and Mt. Yumyeong (the upper left 127°28′45.76074″E, 37°35′59.75109″N and lower right 127°30′6.98627″E, 37°35′6.27425″N), central South Korea. Situated from 160 to 573m above sea level, the study area is dominated by steep hills, with the main tree species being *Pinus koraiensis* (Korean Pine), *Larix leptolepis* (Japanese Larch) and *Quercus* spp. (Oaks), with approximately 1,017.36 ha selected for this study. In the study area,

the PAI_e was measured from 39 plots (13 plots per tree species), and 36 plots (12 plots per tree species) were measured to assess the accuracy. These plots were selected in such a way that the composition of the tree species was homogeneous.

Figure 1. Location of the study areas

3. Acquisition of LiDAR data and ground data

An Optech ALTM 3070 (a small footprint LiDAR system) was used to acquire the LiDAR data. The flight was performed on the 3rd April 2007. The study area was measured at an altitude of 1,400m, with a sampling density of 5~10 points per square meter, with a radiometric resolution, scan frequency and scan width of 12bits, 70Hz and ±20°, respectively. The field survey was performed from the 1st to 4th April, 2008. The number of sample and test plots was 75 (25 plots per tree species). Each plot was 20m x 20m ($400m^2$) in size, and the PAI_e of the plots was measured indirectly using the gap fraction method with an LAI-2000 instrument. The PAI_e was estimated using two LAI-2000 instruments, for the diffuse intensity above and below the canopy. One LAI-2000 used for above the canopy was set up with a 180° view cap on the top of the flux tower. The other LAI-2000 was installed for below-the canopy of the plots. The estimation below the canopy was carried out on the middle spots of each of four edge lines and in four directions from the centre of a square plot with a 180° view cap. The positions of the plots were acquired at breast height in the centre of each plot, using a GPS Pathfinder Pro XR manufactured by the Trimble Corporation.

Table 1. Descriptive statistics of the field measurements

Species	Number of plots	Stand height(m)		Canopy base height (m)		Stand DBH(cm)	
		Mean	Std.	Mean	Std.	Mean	Std.
Pinus koraiensis	25	15.6	2.3	6.8	2.3	32.7	5.5
Larix leptolepis	25	16.4	2.7	6.5	2.0	28.7	4.6
Quercus spp.	25	14.2	2.5	5.5	1.9	28.3	8.9

4. Method

4.1 Potential of using LiDAR for PAI_e estimation

The LiDAR system has the potential for obtaining geo-registered 3D-points; whereas, it is difficult to extract the 3 dimensional information of forested area using independent satellite imagery and aerial photography (Kwak *et al*., 2007). The Laser pulses emitted from the LiDAR system are similar to that of sunlight with respect to the reflectance or transmission through the

canopy. In addition, they are suitable for representing the PAI_e because of the reflectance on the leaves and branches. Therefore, if stands have dense leaves and branches, the LiDAR points are mostly reflected in the canopy. On the other hand, LiDAR points are almost always transmitted to ground due to sparse leaves and branches.

The Beer-Lambert Law has been used to estimate the PAI_e in previous several studies (Pocewicz *et al*., 2004). The PAI_e can be calculated using the Beer-Lambert Law, as shown in equation 1.

$$PAI_e = -\ln(I / I_0) / k_{sun} \quad (1)$$

where I and I_0 are the incident and below-canopy radiation respectively, and k_{sun} is the extinction coefficient for solar radiation. The PAI_e can be estimated using I/I_0, which is known as the gap fraction (G_{sun}), and is defined as the probability of a light beam passing through the canopy without collision (Gower *et al*., 1999). The gap fraction by solar radiation can be alternated with the ratio of the number of LiDAR returns transmitted through the canopy, to the total number emitted from the aircraft (G_{LiDAR}). In equation 1, k_{sun} can be calculated using equation 2 (Campbell, 1986).

$$k_{sun} = \frac{(x^2 + \tan^2\theta)^{\frac{1}{2}}}{x + 1.744(x + 1.182)^{-0.733}} \quad (2)$$

where θ is the zenith angle of the sun and x the leaf angle distribution parameter, which is the ratio of the length of the horizontal to the vertical axes of the spheroid, and can be measured as the ratio of the projected area of an average canopy element onto a horizontal plane to its projection onto a vertical plane (Campbell, 1986). Campbell (1986) suggested that an assumption of an ellipsoidal angle distribution for the canopy elements was most useful. Using such an investigation, x was determined to be 1 when the PAI_e (Campbell labelled this LAI) was estimated in the study area and the angle distribution was assumed to be ellipsoidal. k_{sun} can be simplified to equation 3.

$$k_{sun} = \frac{2}{\cos\theta} \quad (3)$$

In equation 3, k_{sun} could be calculated using the solar zenith angle (θ) in the study area. However, for the PAI_e using LiDAR data, the k_{sun} value must be changed to the zenith angle of the emitted laser pulses from the aircraft (k_{LiDAR}) rather than the solar zenith angle. In this study, the k_{LiDAR} value was estimated using the laser zenith angle (θ) ±10°, which is the median value of the scan angle of every point data reflected in a stand. Therefore, the PAI_e can be estimated from the ratio of the number of transmitted LiDAR returns and the laser zenith angle.

4.2 Classification of LiDAR data using *k*-means statistics

In order to calculate the gap fraction using LiDAR data (G_{LiDAR}), the transmitted laser pulses need to be detected and classified. In particular, the LiDAR returns only intercepted by the canopy must be clustered to estimate the canopy PAI_e only, which is far from the influence of stems among the woody elements, and approximates the LAI despite not including the woody elements of the canopy. Rianõ *et al*. (2004) attempted to test various clustering methods to classify the LiDAR data, such as a 3m fixed limit, minimum Euclidean distance clustering, *k*-means clustering and Expectation Maximization clustering. In this study, *k*-means statistics were used to classify LiDAR data and calculate the gap fraction. The *k*-means statistics is an algorithm used to classify or group attributes or features into k number of groups, and uses an iterative algorithm that

minimizes the sum of the distances (SOD) from each object to its cluster centroid, over all clusters (Equation 4).

$$SOD_{i\ldots j} = \sum_{i}^{j} \left| Centroid_{i\ldots j} - Object[n] \right| \quad (4)$$

This algorithm moves objects between clusters until the sum can be decreased no further. This results in a set of clusters that are as compact and well-separated as possible (MATLAB, 2006). In this study, the number of clusters (k) was determined to be two as to classify LiDAR returns into in-canopy and below-canopy LiDAR returns with the z (height) value of points. The initial points of each cluster can be selected by the user when carrying out k-means clustering. However, in this study, a random selection of k observations from LiDAR point data was used, with 100 iterations calculated. Moreover, the cluster was treated as an error if it was too small, e.g., the percentage of laser pulses of a group had less than 1/(total number of clusters)^2 (Rianõ *et al*., 2004). Thereby, the laser interception indices (LII) according to the tree species was generated using the LiDAR returns reflected through the canopy.

4.3 Generation of Laser Interception Index

Barilotti *et al*. (2006) suggested the use of the laser penetration index (LPI), with the point density of the ground returns and vegetation returns in the sample plots. All LiDAR points were divided into two classes; high (height ≥ 1m above ground), and low (height < 1m above ground) vegetation returns. However, in the case of various heights of the understory, the LPI was not flexible because the value used to distinguish the ground and high vegetation returns was fixed at a height 1m above the ground regardless of the characteristic of the forest stand. Therefore, the LII was calculated in order to apply flexible heights considering the characteristics of various forest stands, as shown in equation 5.

$$LII = \frac{N_{in\ canopy\ returns}}{N_{total\ returns}} = 1 - \frac{N_{below\ canopy\ returns}}{N_{total\ returns}} \quad (5)$$

where $N_{in\ canopy\ returns}$ is the number of LiDAR returns intercepted by the canopy, $N_{below\ canopy\ returns}$ is the number of LiDAR returns transmitted through the canopy and $N_{total\ returns}$ is the total number of LiDAR returns emitted from the aircraft. According to equation 5, the vegetation is dense if the value of LII is close to 1, but the vegetation is sparse if the value is close to 0. Incidentally, the LII is an opposite concept, which is related to the ground covered by the canopy, even when the LiDAR gap fraction (G_{LiDAR}), which is the ratio of transmitted LiDAR returns to the total LiDAR returns, is need to calculate PAI_e. Therefore, equation 5 must be changed into equation 6 in order to apply LII to the PAI_e.

$$G_{LiDAR} = \frac{N_{below\ canopy}}{N_{total\ returns}} = 1 - LII \quad (6)$$

Finally, the PAI_e can be estimated artificially by the tree species by substituting G_{sun} and k_{sun} for G_{LiDAR} and k_{LiDAR}, respectively as shown in equation 7.

$$PAI_e = -2\cos\theta_{LiDAR} \cdot \ln(1 - LII) \quad (7)$$

5. Result and discussion

5.1 Classification of LiDAR data

As a result of the classification of the LiDAR returns using *k*-means clustering, the LiDAR returns by the tree species were classified into two clusters as shown in figure 3, because the LiDAR returns for both *Pinus koraiensis* and *Larix leptolepis* were almost reflected in the canopy and ground due to the dense leaves and branches with rare understories. *Quercus* spp. could also be divided into two clusters due to the larger number of ground returns than above ground returns. Figure 3 shows the typical distribution of the LiDAR returns according to the species of tree.

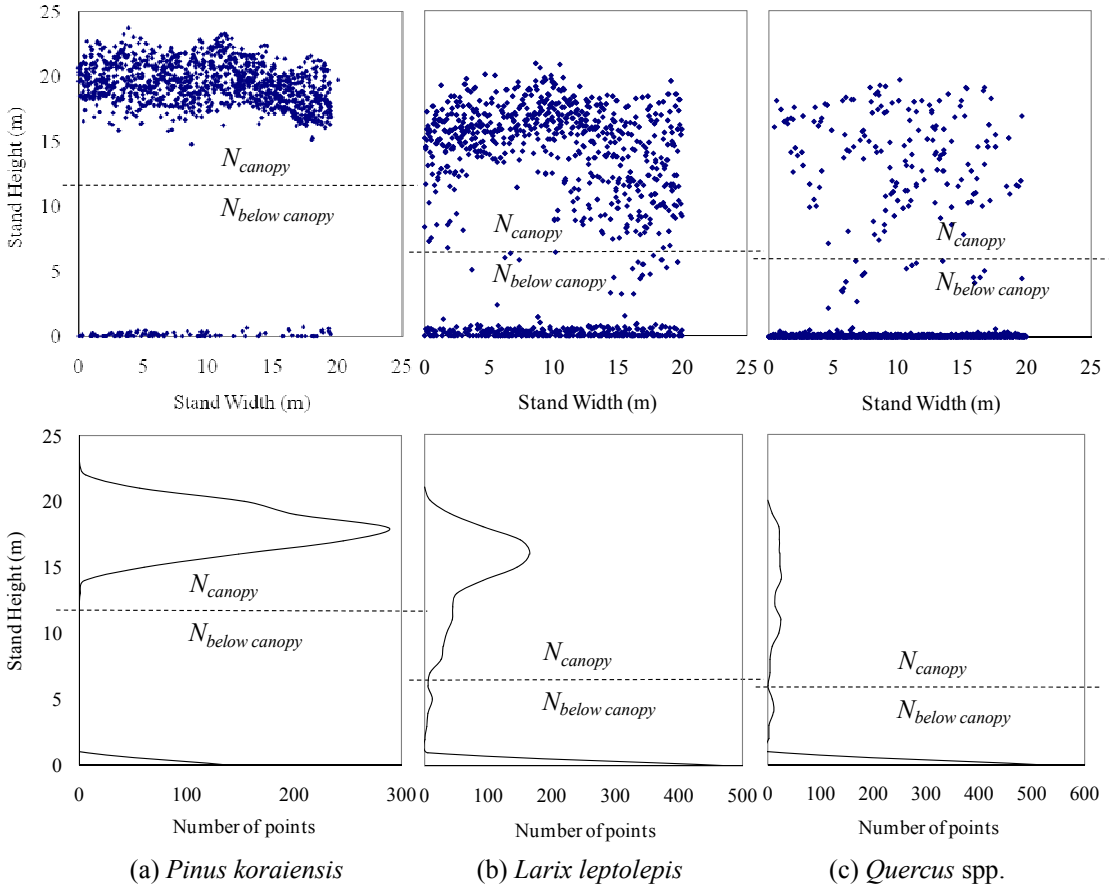

Figure 3. Distribution of the LiDAR returns and classification into two clusters by the tree species

The LiDAR data was partitioned into two groups, and then G_{LiDAR} was generated using N_{canopy}, $N_{below\ canopy}$ and N_{all}. Because few understories existed and abundant canopy in the plots for *Pinus koraiensis*, the LiDAR returns could be clearly clustered into two groups, without a middle point layer. However, some of the LiDAR pulses in the plots for *Larix leptolepis* and *Quercus* spp. were reflected in a middle point layer because there were some understories and no leaves when the field survey was carried out. Nevertheless, the results of *k*-means statistics with two centroids were acceptable because the threshold heights for classifying the in-canopy and below-canopy points were similar to the field-derived crown base heights, which were 6.5 and 5.5m for *Larix leptolepis* and *Quercus* spp., respectively. In particular, the LiDAR returns in the plots for *Quercus* spp. were clustered well into two parts, even with abundant LiDAR returns on the ground and a few on the branches as a result of the species having few leaves. These classification results were used to estimate the LiDAR-derived LAI using G_{LiDAR}.

5.2 Estimation of effective plant area index using LiDAR gap fraction

Using the G_{LiDAR} values, the LiDAR-derived PAI_es, which mean the only canopy PAI_es, were estimated by tree species. The PAI_es of *Pinus koraiensis* were higher than those of *Larix leptolepis* and *Quercus* spp., because it is an evergreen needle tree with dense leaves. On the other hand, the PAI_es of *Larix leptolepis* and *Quercus* spp. were relatively low because they had a few leaves and branches when the field survey was carried out, i.e. from 1st to 4th April. However, The PAI_es of *Larix leptolepis* were much higher than those of *Quercus* spp.. This was attributed to the emitted LiDAR pulses being reflected on the many dense branches of *Larix leptolepis,* as shown in Figure 4.

(a) *Pinus koraiensis* (b) *Larix leptolepis* (c) *Quercus* spp.

Figure 4. Structure of the stands surveyed by tree species

Linear regression analysis was carried out to determine the relationship between the LiDAR-derived and field-derived PAI_e. The coefficient of determination (R^2) and root mean square error (RMSE) were calculated to determine the accuracy of the estimated regression analysis (Table 2).

Table 2. Accuracy of the regression function generated by LPI and LII

Tree species	Statistics	Results
Pinus koraiensis	Function	$PAI_e = -0.629 \cdot \frac{\ln(G_{LiDAR})}{k} + 1.490$
	R^2	0.75
	RMSE	0.40
Larix leptolepis	Function	$PAI_e = -0.404 \cdot \frac{\ln(G_{LiDAR})}{k} + 1.694$
	R^2	0.89
	RMSE	0.42
Quercus spp.	Function	$PAI_e = -0.595 \cdot \frac{\ln(G_{LiDAR})}{k} + 0.983$
	R^2	0.65
	RMSE	0.52

As a result, the accuracy for *Pinus koraiensis* was the highest of the three tree species, because

the LiDAR returns were mostly reflected through the canopy and rarely onto the ground without a middle point layer, which is similar to the transmission of solar radiation, because the stands of *Pinus koraiensis* have dense leaves. A greater number of LiDAR returns reflected in the canopy can provide a better description of the canopy. On the other hand, *Quercus* spp. showed only a slight relationship between the estimates and ground truth data, which was attributed to *Quercus* spp. having no leaves and a few branches on the tree stems compared with *Larix leptolepis*. No leaves on branches caused some estimation errors due to direct sunlight being sensed into the LAI-2000 or the other instruments when the PAI_e is measured. Therefore, *Quercus* spp. with no leaves and a few branches had fluctuating PAI_es. The PAI_e of *Larix leptolepis* was more stable because the abundant branches play the role of leaves.

5.3 Accuracy assessment

The PAI_es estimated by regression analysis were evaluated using the field-derived PAI_es in 36 plots (12 plots by tree species) selected for verification. The accuracies for *Pinus koraiensis, Larix leptolepis* and *Quercus* spp. were 0.82, 0.71 and 0.54, respectively (Figure 5).

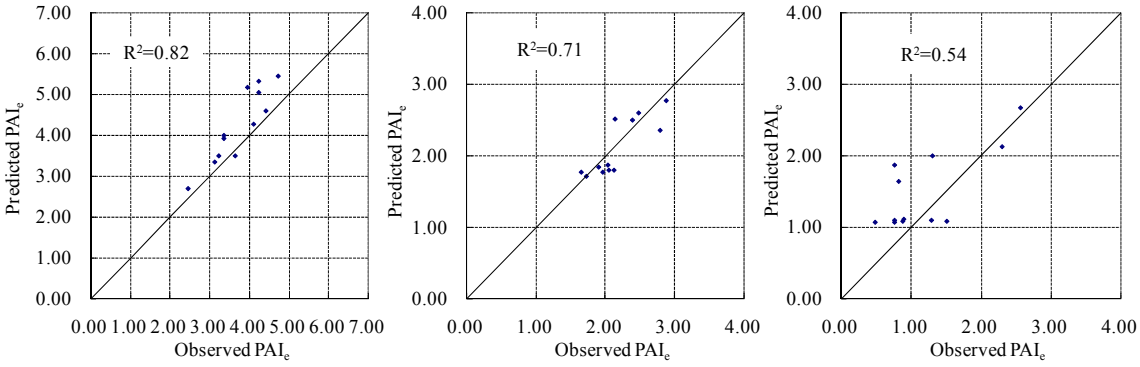

(a) *Pinus koraiensis* (b) *Larix leptolepis* (c) *Quercus* spp.

Figure 5. Evaluation of the estimated LAI analysis by the tree species

The estimated PAI_es of *Pinus koraiensis* had the highest R^2 of the three tree species. This is due to the right measurement without the direct sunlight because *Pinus koraiensis* had abundant leaves on the branches. Moreover, the predicted PAI_e were mostly higher than the observed PAI_es in the test plots. This was attributed to the different amounts of understory between the sample and test areas. Namely, the understory of the test plots might have been less than that in the sample area. The estimated PAI_es for *Larix leptolepis* were relatively accurate due to the abundant branches, even though there were few leaves on the trees. The plenty branches decrease the estimation errors with LAI-2000 because they diffuse direct sunlight. Therefore, the accuracy for *Quercus* spp. was the lowest of the three tree species due mainly to the estimation errors with LAI-2000. The lack of leaves and the poor vertical distribution of the branches might have caused the poor results. When the PAI_es were measured in the *Quercus* spp. stands, the direct sunlight penetrating through the canopy influenced the actual PAI_es because LAI-2000 the recorded mixed value of the diffused radiation and direct sunlight in forested areas. Therefore, LAI-2000 has a weak point in that PAI_es need to be measured around sunrise or sunset. During Summer or early Autumn, the accuracy of the regression function and its evaluation should increase due to the larger number of laser pulses reflected on the leaves as well as the diffusion of direct sunlight by the leaves through the canopy for *Larix leptolepis* and *Quercus* spp.. The PAI_es estimation of trees without leaves, i.e. deciduous trees in late Autumn and early Spring, may be invalid from the point of view of evaluating the PAI_es for trees with the best leaves. However, such research may be valuable because the change in the amount of leaves can be monitored according to season.

The k_{LiDAR} derived using the LiDAR zenith angle and leaf angle distribution also plays an important role in assessing the accuracy. Indeed, each zenith angle of the LiDAR returns reflected in a forest stand has independent values because each LiDAR pulse is emitted from the respective angles due to the rotation of the sensor mounted in the LiDAR system. Therefore, the zenith angles of all the LiDAR returns of a target forest stand need to be detected and calculated for more accurate results when estimating the PAI_e from LiDAR data. In addition, the leaf angle distribution should to be also applied with respect to the tree species, even though the leaf angle distribution in this study was assumed to have a value of 1, which suggests an ellipsoidal angle distribution. In future studies, three variables, the LII, laser zenith angle and leaf angle distribution must be considered for more reasonable and precise estimates of the PAI_e using LiDAR data.

6. Conclusion

The LAI was estimated using the laser interception index for three tree species, *Pinus koraiensis*, *Larix leptolepis* and *Quercus* spp.. In the PAI_es equation by the Beer-Lambert Law, the gap fraction (I/I_0) for the sun was replaced by G_{LiDAR}, which is the ratio of the number of below-canopy points to that of all returns in the sample plots. The G_{LiDAR} was calculated by classifying the in-canopy and below-canopy points using *k*-means statistics. In the Beer-Lambert Law, the k_{sun} extinction coefficient was calculated using the solar zenith angle and leaf angle distribution. However, instead of k_{sun}, k_{LiDAR} could be generated using the laser zenith angle (±10°, median value of every point in sample plots) and leaf angle distribution (x=1, meaning of ellipsoidal leaf angle distribution). As a result, the coefficient of determination between the observed and predicted PAI_e for *Pinus koraiensis*, *Larix leptolepis* and *Quercus* spp. were 0.82, 0.71 and 0.54, respectively. When the PAI_es are acquired in forest stands with few leaves and poor branches, such as deciduous trees in spring or winter, direct sunlight affects the estimation because the optical sensors, e.g. LAI-2000 and AccuPAR-80, measure the diffused radiation transmitted through the canopy. Therefore, the reason for the different PAI_e with regard to tree species was that *Larix leptolepis* and *Quercus* spp. had no leaves, and *Pinus koraiensis* had abundant leaves. The accuracy for *Larix leptolepis* was higher than that of *Quercus* spp. which is because *Larix leptolepis* has more abundant branches that play a role of diffusing the direct sunlight, while *Quercus* spp. had a poor branch distribution vetically. Therefore, with *Larix leptolepis* and *Quercus* spp., more accurate results than those found in this study are expected if the study is performed in late spring when their shoots and leaves begin to appear. The k_{LiDAR} derived using the LiDAR zenith angle and leaf angle distribution also plays a role in estimating the PAI_e using LiDAR data. Even when fixed values for the laser zenith angle and leaf angle distribution are used, future investigations should consider the actual laser zenith angles of each point in the target forest stands and the leaf angle distribution according to the tree species.

Acknowledgements

The authors wish to thank Kang-Won Lee, Managing Director of Hanjin Information System and Telecommunication Corporation, South Korea, for providing the LiDAR data.

References

Barilotti, A., Turco, S. and Alberti, G., 2006. LAI determination in forestry ecosystem by lidar data analysis, *Proceedings of Workshop on 3D Remote Sensing in Forestry*, Vienna, Austria: 248-252.

Bonan, G. B., 1993. Importance of leaf area index and forest type when estimating photosynthesis in boreal forsts. *Remote Sensing of Environment*, 43, 303-314.

Bréda, N. J. J., 2003. Ground-based measurements of leaf area index: a review of methods, instruments and current controversies. *Journal of Experimental Botany*, 54, 2403-2417.

Campbell, G. S., 1986. Extinction coefficients for radiation in plant canopies calculated using an ellipsoidal inclination angle distribution. *Agricultural and Forest Meteorology*, 36, 317-321.

Chen, J. M. and Cihlar, J., 1996. Retrieving leaf area index of boreal conifer forests using Landsat TM images. Remote Sensing of Environment, 55, 153-162.

Cohen, W. B., Maiersperger, T. K., Gower, S. T. and Turner, D. P., 2003. An improved strategy for regression of biophysical variables and landsat etm+ data. *Remote Sensing of Environment*, 84, 561-571.

Gower, S. T., Kucharik, C. J. and Norman, J. M., 1999. Direct and indirect estimation of leaf area index, fAPAR, and net primary production of terrestrial ecosystems, *Remote Sensing Environ,* 70, 29-51.

Holmgren, J., Nilsson, M. and Olsson, H., 2003. Estimation of tree height and stem volume on plots using airborne laser scanning. *Forest Science*, 49, 419-428.

Jonckheere, I., Fleck, S., Nackaerts, K., Muys, B., Coppin, P., Weiss, M. and Baret, F., 2004. Review of methods for in situ leaf area index determination: Part i. theories, sensors and hemispherical photography. *Agricultural and Forest Meteorology*, 121, 19-35.

Koetz, B., Schaepman, M., Morsdorf, F., Itten, K. and Allgöwer, B., 2004. Radiative transfer modeling within a heterogeneous canopy for estimation of forest fire fuel properties. *Remote Sensing of Environment*, 92, 332-344.

Koetz, B., Morsdorf, F., Sun, G., Ranson, K. J., Itten, K. and Allgöwer, B., 2006. Inversion of a lidar waveform model for forest biophysical parameter estimation. *IEEE Geoscience and Remote Sensing*, 3, 49-53.

Kwak, D. A., Lee, W. K., Lee, J. H., Biging, G. S. and Gong. P., 2007. Detection of individual trees and estimation of tree height using LiDAR data, *Journal of Forest Research*, 12, 425-434.

MATLAB, 2006, Help document in program. Mathwork, United States of America.

Morsdorf, F., Kötz, B., Meier, E., Itten, K. I. and Allgöwer, B., 2006. Estimation LAI and fractional cover from small footprint airborne laser scanning data based on gap fraction. *Remote Sensing of Environment*, 104, 50-61.

Myneni, R., Nemani, R. and Running, S., 1997. Estimation of global leaf area index and absorbed par using radiative transfer models. *IEEE Transactions on Geoscience and Remote Sensing*, 35, 1380-1393.

Pocewicz, A. L., Gessler, P. and Robinson A. P., 2004, The relationhip between effective palnt area index and Landsat spectral response across elevation, solar insolation, and spatial scales in a northern Idaho forest. *Canadian Journal of Forest Research*, 34, 465-480.

Riaño, D., Valladares, F., Condés, S. and Chuvieco, E., 2004, Estimation of leaf area index and covered ground from airborne laser scanner (Lidar) in two contrasting forests. *Agricultural and Forest Meteorology*, 124, 269-257.

Schulze, E. D., Beck, E., Müller-Hohenstein, K., Lawlor, D., 2005. Plant ecology, Springer (eds)., Berlin.

Watson, D. J., 1947. Comparative physiological studies in the growth of field crops. I. Variation in net assimilation rate and leaf area between species and varieties, and within and between years. *Annals of botany*, 11, 41-76.